Journal of Thermal Analysis and Calorimetry (2022) 147:4925–4934
https://doi.org/10.1007/s10973-021-10886-0

Design of n-octadecane-based form-stable composite phase change materials embedded in porous nano alumina for thermal energy storage applications

Hatice Hande Mert[1] · Mehmet Selçuk Mert[2]

Received: 16 November 2020 / Accepted: 2 May 2021 / Published online: 26 May 2021

Abstract
A new shape-stabilized composite phase change material (SSCP) was fabricated by using a promising matter, namely n-octadecane (n-OD) having 200–244.00 kJ kg^{-1} thermal energy storage capacity. For this aim, one step impregnation method was conducted in order to obtain the composite PCM. Nano-sized gamma alumina (γ-Al_2O_3) was used as the support material that enhances the thermal properties of the smart composite. The obtained composite materials were investigated by thermal analyse and visualization methods in order to determine its thermal energy storage capacity, phase transition temperature, thermal stability, chemical structure and morphology based on the differential scanning calorimetry (DSC), thermogravimetric analysis (TGA), Fourier transform infrared spectroscopy and polarized optical microscopy analyses, respectively. Based on the DSC results, composite SSCP4 which could be obtained by using a composition of n-OD/γ-Al_2O_3 of 50:50 (mass/%) has highest thermal energy storage capacity (86.00 J g^{-1}) with the suitable transition temperature (18.95–27.40 °C). Moreover, impregnation ratio of n-OD into the porous framework was found to be 39.58 (mass/%) by TGA. Accordingly, the obtained composite PCM can be a promising candidate for low-temperature (18–30 °C) thermal applications which are required to have the favorable phase change temperature and high energy storage capacity with thanks to its good thermal stability and durability performance.

Keywords n-octadecane · Gamma alumina · Composite phase change material · Energy storage

Introduction

Phase change materials (PCMs) are significant substances that allow achieving energy efficient designs via thermal energy storage. By using these materials, the latent heat energy of the material can be stored/released when the convenient conditions achieved [1]. Phase change materials are also called as smart materials owing to its phase transition behavior depending on the ambient temperature without any external intervention [2].

✉ Mehmet Selçuk Mert
msmert@yalova.edu.tr

Hatice Hande Mert
hndmert@yalova.edu.tr

[1] Faculty of Engineering, Department of Chemical Engineering, Yalova University, 77200 Yalova, Turkey

[2] Faculty of Engineering, Department of Energy Systems Engineering, Yalova University, 77200 Yalova, Turkey

Porous materials are extensively preferred many applications such as catalysis, adsorption due to their attractive properties like large specific surface area, high porosity and pore volumes, superior heat and mass transfer properties. Porous materials can also use as support matrix for bounding organic-based latent heat storage materials to overcome leakage problem during the phase transition [3, 4]. Synergetic combination of porous templates and PCMs via shape-stabilization approach not only prevents the leaking of melted phase, but also improve some properties such as thermal and chemical stability and durability besides to ensure high thermal energy storage density [5]. Porous carbon, graphite scaffolds, polyurethane foams, silica scaffolds and clays are the porous materials used for shape stabilization of PCMs [6, 7]. Moreover, metal foams such as copper [8, 9], nickel [9], aluminum [10] with thanks to desirable skeleton structure and high thermal conductivity have been used as support for shape-stabilization of PCMs.

Organic, inorganic and eutectic types of PCMs are extensively used in thermal energy storage applications [11, 12].

For this purpose, paraffins that are in the organic materials class are also highly preferred [13]. Among them, n-octadecane has been investigated by many scientists due to its favorable thermal energy storage capacity (200–244.00 kJ kg^{-1}) and phase transition temperature (28–28.4 °C). When the literature is examined, it has been seen that the preparation of micro/nano-encapsulated, emulsion type and form stable PCMs containing n-octadecane has been studied [13–15]. Ho and Gao performed the dispersion of 5 mass/% and 10 mass/% alumina nanoparticles in n-octadecane in order to obtain emulsion type phase change material. They concluded that the addition of Al_2O_3 had no significant effect on the phase change temperatures of the PCM, and it was observed around 26 °C and 25 °C, respectively, for melting and freezing processes. The latent heat of fusion of the obtained PCMs was found as 243.1 kJ kg^{-1}, 225.6 kJ kg^{-1} and 212.3 kJ kg^{-1}, respectively, for mass/0%, mass/5% and mass/10% [16]. Fang et al. carried out the preparation of palmitic acid/ active aluminum oxide composites as form stable phase change material. Aluminum oxide (average particle diameter: 3–5 mm) was chosen as the support material for obtaining the composite PCM while the fatty acid percentage (mass/%) was 45%. The latent heat of fusion and crystallization was obtained as 84.48 kJ kg^{-1} and 78.79 kJ kg^{-1} while the phase transition temperatures were 60.25 °C and 56.86 °C, respectively [17]. Wei et al. studied the fabrication of fatty acid mixture/expanded vermiculite phase change material with and without alumina addition. Eutectic mixture of lauric, myristic and stearic acids having 59.5:32.0:8.5 mass percentages was prepared and used as the PCM. The latent heat of fusion of the obtained composites was 91.6 kJ kg^{-1} and 113.7 kJ kg^{-1} for with and without alumina, respectively, while the melting temperature was measured as about 28 °C. They noted that the doping of alumina into the expanded vermiculite enhanced the thermal conductivity of the composite PCM [18]. Zhao et al. [19] studied the microencapsulation of n-octadecane with TiO_2 shell via sol–gel method. They obtained spherical-shaped microcapsules having 42.57 J g^{-1} thermal energy storage capacities with a melting temperature around 25 °C. Furthermore, it was noted that the use of TiO_2 shell exhibited a good thermal stability. In a previous work of us, a paraffin mixture composed of n-octadecane and n-hexadecane with poly(St-co-DVB) shell were prepared by inverse emulsion polymerization [20]. According to the findings, the phase change temperature and the latent heat of melting of the microPCM were found as 21.06 °C and 88 kJ kg^{-1}, which were reported as a suitable material for low level thermal storage applications based on the good thermal stability of the obtained PCM [20]. In another work, a fatty acid mixture besides to n-hexadecane was microencapsulated with the addition of modified gamma alumina in order to improve the thermal conductivity of the composite PCM. The supplement of 2% γ-Al_2O_3 into the composite lead the enhancement of the heat transfer rate by 6.23% while the latent heats of fusion/crystallization declined with the increasing load amounts of M-γ-Al_2O_3 [21].

To the best of our knowledge until today, no study has been reported on n-octadecane impregnation into nano-sized γ-Al_2O_3 (< 50 nm) used as supporting material for developing shape-stabilized composite PCM. Hence, in the present study, it was aimed to obtain n-octadecane/γ-Al_2O_3 composite phase change material by one-step impregnation method for low-temperature heat storage applications. The shape-stabilized composite PCMs (SSCPs) were prepared by one step impregnation method at different compositions, and their thermal properties besides to thermal energy storage capacity were investigated. Commercially purchased nano gamma alumina used as framework due to its superior properties such as large specific surface area and suitable pore volume, while the n-octadecane selected as PCM with thanks to high latent heat storage capacity and favourable phase transition temperatures. Firstly, the latent heat storage capacity and phase transition temperatures of produced SSCPs, which are crucial for thermal energy storage applications, were determined by DSC. Then the composite material which has the highest thermal energy storage capacity was selected. Its thermal stability by TG, the chemical structure by FT-IR, the morphologic characterization by POM and durability by leakage test were investigated. Moreover, demonstration of thermal performance of composite phase change material being one of the aim of this work was tested in a in a system which was equipped with temperature controlled circulating bath and data logger. Consequently, producing of a shape-stabilized composite material, which has improved durability performance, thermal and chemical stability via combination of porous nano alumina as a support material and n-octadecane as a PCM is the main objective of this study.

Materials and method

Materials and characterization

n-octadecane (n-OD) (paraffin, Merck, Darmstadt, Germany) as a PCM and gamma phase alumina nano powder (nanoparticle, < 50 nm, Sigma-Aldrich) as a framework were used as purchased.

The thermogravimetric analysis (TGA) of the n-OD, pure gamma alumina (γ-Al_2O_3) and shape stabilized composite PCM (SSCP) were carried out with a thermal analyzer (Seiko TG / DTA 6300 thermal analysis system instrument, Seiko Instruments, Tokyo, Japan) at a heating rate of 10 °C min^{-1} under nitrogen atmosphere. FT-IR spectra of the n-OD, pure gamma alumina (γ-Al_2O_3) and shape stabilized composite

PCM (SSCP) were obtained by Perkin Elmer, Spectrum 100 FT-IR spectrophotometer at a wavelength of 650–4000 cm^{-1} at room temperature. Determination of the melting temperature (T_m), crystallization temperature (T_c), latent heat of melting (ΔH_m) and latent heat of crystallization (ΔH_c) of PCMs were conducted with Differential Scanning Calorimetry (DSC 7020 HITACHI) under nitrogen atmosphere and at 5 °C min^{-1} heating rate. The incorporation rate (mass/%) of n-OD in the γ-Al_2O_3 skeleton was calculated using the following equation [1]:

$$\text{n-OD content in composite (mass/\%)} = \frac{\Delta H_{SSCP}}{\Delta H_{n\text{-}OD}} \times 100$$

here in, ΔH_{SSCP} is the latent heat of melting of shape-stabilized composite containing n-OD (J g^{-1}), and $\Delta H_{n\text{-}OD}$ is the latent heat of melting of pure n-OD without supporting material (J g^{-1}).

The morphological characterization of the neat gamma alumina (γ-Al_2O_3) and SSCP was examined by POM (Leica DM2700P polarizing microscope). Specific surface area, pore volume and pore size of gamma alumina (γ-Al_2O_3) were determined by applying Brunauer–Emmet–Teller (BET) and Barrett-Joyner-Halenda (BJH) model equations on N_2 adsorption/desorption isotherms, respectively. For this purpose, Micromeritics Gemini VII 2390 t Overall Automatic Surface Area and Porosity Analyzer (Micromeritics Instrument Corporation, USA) was used. Prior to analysis the sample was degassed at 100 °C for 24 h on a Micromeritics FlowPrep 060 Sample Degas System (Micromeritics Instrument Corporation, USA).

Thermal behaviors of samples during cooling process were also investigated in a system which was equipped with temperature controlled circulating bath and data logger. For this aim, samples were placed into test tubes and immersed in the bath, which was filled with ethanol as a heat transfer liquid. The bath was cooled from 40 to 15 °C, which temperature range was comprised the crystallization temperature of PCM.

Experimental

Preparation of shape-stabilized composite PCMs (SSCPs)

Shape-stabilized n-OD/γ-Al_2O_3 composite PCMs were prepared by one step impregnation method [1] in accordance with the compositions given in Table 1. The nano sized powder γ-Al_2O_3 was dried in a vacuum oven at 110 °C for 24 h for removing moisture in its pores. n-OD was placed in a glass reactor and heated to 35 °C above its melting temperature. 50 mL ethanol was added into melted n-OD and stirred at 35 °C for 30 min. The n-OD solution was poured onto a certain amount of powder γ-Al_2O_3, and mixture was homogenized in an ultrasonic bath at 35 °C for 30 min. After that, n-OD/γ-Al_2O_3 solution mixed with a mechanical stirrer at 350 rpm for 24 h at temperature above melting temperature of n-OD. At the end of the mixing process, solution was placed in a vacuum oven, and ethanol was removed at 80 °C for 24 h. The obtained composites were called as SSCP.

Table 1 The composition of shape-stabilized composite PCMs (SSCPs) prepared by one step impregnation method

Samples	γ-Al_2O_3 (mass/%)	n-OD (mass/%)
SSCP1	80	20
SSCP2	70	30
SSCP3	60	40
SSCP4	50	50

Results and discussion

Nitrogen adsorption–desorption

The porous nano materials are frequently preferred as a template due to their ideal surface area in order to form-stable PCMs. The N_2 adsorption/desorption isotherm of gamma alumina was illustrated in Fig. 1 while the measured properties such as BET spesific surface area, pore volume and pore diameter were also given in Table 2. As shown in Fig. 1, N_2 adsorption–desorption isotherm of γ-Al_2O_3 which exhibited adsorption hysteresis loop at the range of relative pressure (p/p^0) of 0.9–1.0 was coherent with typical type IV isotherm. Thus, it could be said that type IV isotherm of γ-Al_2O_3 was consistent with mesoporous structure of it [22, 23]. BET specific surface area of γ-Al_2O_3 was found to be as 145.92 m^2 g^{-1} while the BJH adsorption cumulative volume of pores and BJH adsorption average pore width were determined as 1.51 cm^3 g^{-1} and 34.80 nm, respectively (Table 2). The large pore volume and pore width of the γ-Al_2O_3 were advantageous for n-OD to easily integration into the γ-Al_2O_3 pores.

Thermal properties and latent heat storage capacities of shape-stabilized composite PCMs (SSCPs)

DSC curves of n-OD and SSCPs acquired during melting and crystallization were given in Fig. 2, and the data obtained from DSC curves were presented in Table 3. As seen from the Fig. 2, the presence of melting and crystallization peaks affirm that the impregnation of n-OD into the gamma alumina framework. As expected (Table 3), latent heat of melting (ΔH_m) and latent heat of crystallization (ΔH_c) values of composite PCMs were declined in comparison with unconstrained n-OD due to impregnation of n-OD into the nano alumina skeleton. Although melting

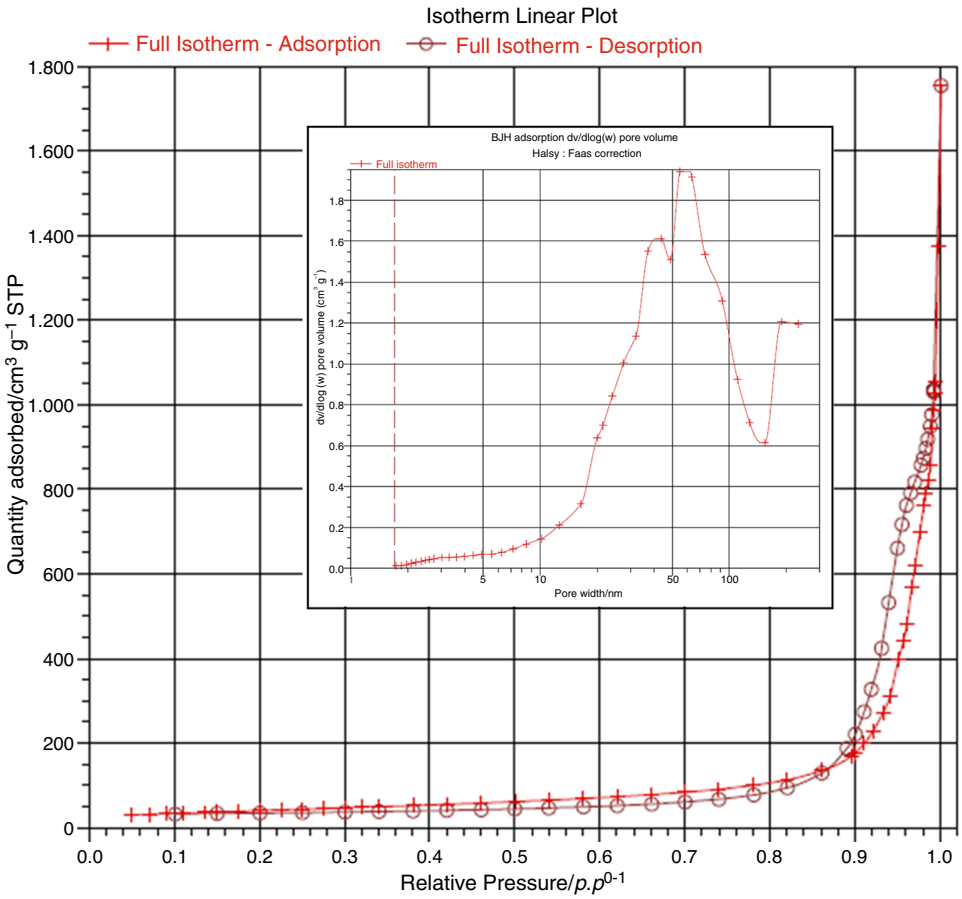

Fig. 1 N_2 adsorption–desorption isotherm of the nano gamma alumina

Table 2 The measured properties of nano gamma alumina

Gamma Alumina (γ-Al_2O_3)	
BET surface area ($m^2\ g^{-1}$)	145.92
BJH adsorption cumulative volume of pores ($cm^3\ g^{-1}$)	1.51
BJH adsorption average pore width (nm)	34.80

temperatures during heating and crystallization temperatures during cooling also decreased by comparison to n-OD, these values generally increased by increment n-OD content. As also seen from Table 3, the latent heat of melting of samples was found to be 220.0 J g^{-1}, 28.60 J g^{-1}, 31.30 J g^{-1}, 63.30 J g^{-1} and 86.00 J g^{-1} for n-OD, SSCP1, SSCP2, SSCP3 and SSCP4, respectively.

Moreover, the calculated n-OD contents in SSCP1-SSCP4 according to Eq. (1) were found to be 13.00%, 14.22%, 28.77% and 39.09%, respectively, although theoretical PCM contents were to be 20%, 30%, 40% and 50% in corresponding recipes (Table 1). This difference could be attributed to restriction of the molecular chains of n-OD by the drag and steric effects of the mesopores of γ-Al_2O_3 [24]. Moreover, γ-Al_2O_3 has mesoporous structure with different pore size distribution as given in Fig. 1. The pore structure of γ-Al_2O_3 could have effect on the phase transitions of n-OD filled in the pores because of the capillary and surface tension forces between the n-OD and pores. It could be caused to inhibiting the molecular mobility of n-OD during the phase transitions [25, 26]. As a consequence of this phenomena, n-OD content which calculated from the enthalpy values measured by DSC being lower than theoretical values.

It can be safely stated that from the DSC results that SSCP4 has the highest latent heat storage capacity as a result of having the highest n-OD content. Accordingly, among the composite materials, SSCP4 with the highest thermal energy storage capacity (86.00 J g^{-1}) is a good candidate as a shape-stabilized composite PCM with the suitable transition temperature (18.95–27.40 °C) for low temperature (18–30 °C) thermal energy storage applications. Moreover, Table 4 presents the comparison of shape-stabilized composite phase change materials prepared by using porous materials in literature [27–35]. According to this table, SSCP4 as a shape-stabilized n-OD/nano gamma alumina composite phase change material has a remarkable potential owing to latent heat capacity for the thermal energy storage applications.

The thermal stability of obtained composite SSCP4 was also investigated by TGA. TG curves of n-OD, γ-Al_2O_3 and SSCP4 were given in Fig. 3. As seen from the TG curves,

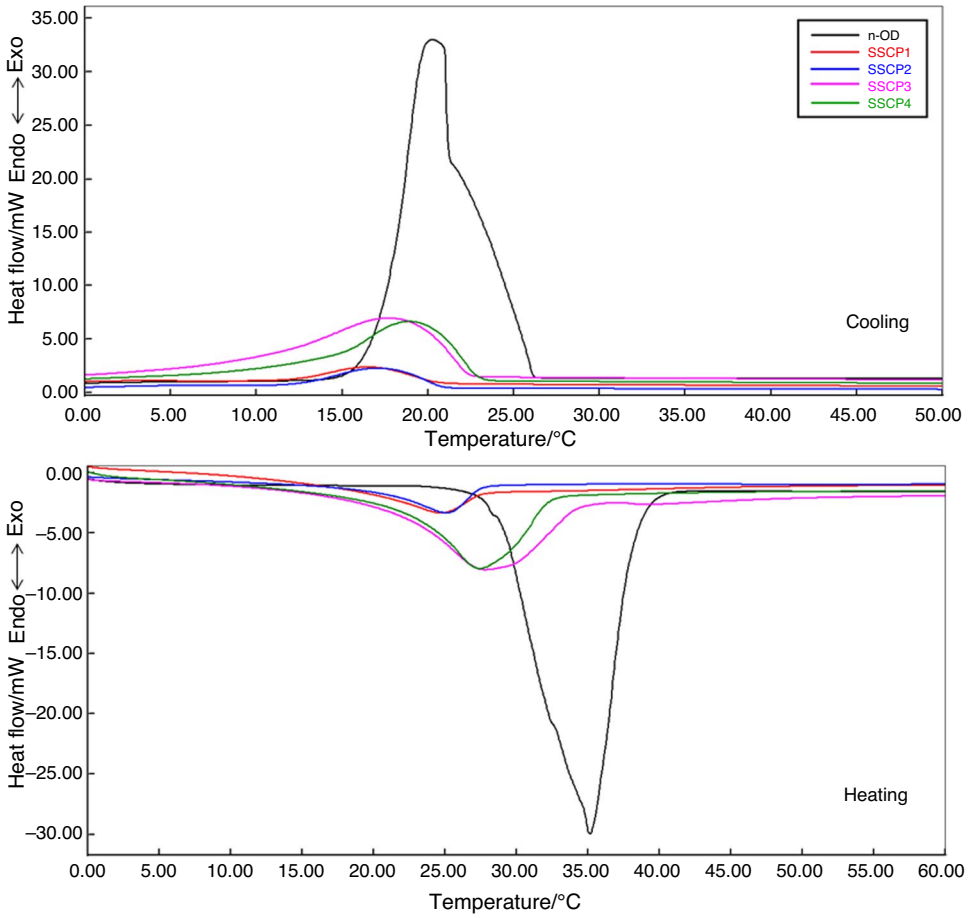

Fig. 2 DSC curves of the n-OD and shape-stabilized composite PCMs (SSCPs)

Table 3 DSC data of the n-OD and SSCPs

Sample	T_{om}/°C[a]	T_{pm}/°C[b]	T_{em}/°C[c]	ΔH_m/J g^{-1}[d]	T_{oc}/°C[e]	T_{pc}/°C[f]	T_{ec}/°C[g]	ΔH_c/J g^{-1}[h]	n-OD content (mass%)
n-OD	28.54	35.16	38.41	220.0	22.08	20.31	17.01	− 218.0	100
SSCP1	17.19	24.71	27.54	28.60	20.70	16.58	12.00	− 15.30	13.00
SSCP2	19.70	25.09	27.63	31.30	20.87	17.09	12.15	− 19.70	14.22
SSCP3	20.56	27.79	34.04	63.30	22.31	17.79	9.50	− 59.30	28.77
SSCP4	21.93	27.40	32.34	86.00	22.91	18.95	13.53	− 68.70	39.09

[a]Onset melting temperature during heating
[b]Peak melting temperature during heating
[c]Endset melting temperature during heating
[d]Latent heat of melting
[e]Onset crystallization temperature during cooling
[f]Peak crystallization temperature during cooling
[g]Endset crystallization temperature during cooling
[h]Latent heat of crystallization

one step-degradation process was obtained for n-OD in the temperature range of 145 °C to 228 °C with the mass loss of 98.5, whereas mass loss of pure nano gamma alumina used as supporting material was found to be as 5.2% at near 100 °C due to the removal of present moisture in structure. Moreover, nano γ-Al_2O_3 was maintained its thermal stability until at 600 °C without any thermal degradation. Furthermore, SSCP4 composite which has the

Table 4 Comparison of different composite PCMs available in the literature

Composite PCM	Melting temperature/°C	Latent heat of melting/J g^{-1}	Reference
Paraffin RT20/montmorillonite	20.8	53.6	[27]
Stearic acid/graphene-decorated silica	51.5	51.3	[28]
Paraffin RT21/expanded perlite	22.1	60.9	[29]
Paraffin/bentonite	44.3	39.8	[30]
Capric-myristic acid/vermiculite	23.3	27.4	[31]
n-octadecane/TiO_2	28.2	85.8	[32]
n-octadecane/meso-porous carbon	13.5	18.6	[33]
n-heptadecane/biochar	13.9	53.3	[34]
n-heptadecane/activated carbon	14.1	85.4	[34]
Capric acid-stearic acid/silica fume	23.2	65.6	[35]
n-octadecane/gamma nano alumina	27.4	86.0	This study

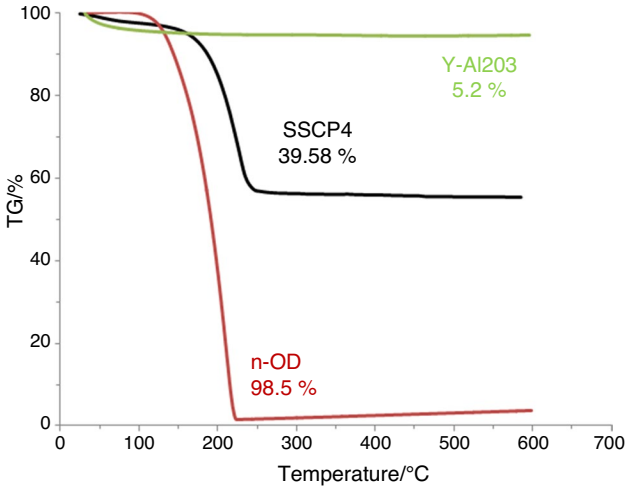

Fig. 3 TG curves of the n-OD, γ-Al_2O_3 and SSCP4

highest latent heat storage capacity exhibited degradation until to 245 °C which corresponds to evaporation/decomposition of the n-OD. It could be clearly seen from the TG curve of SSCP4 that degradation of n-OD which was in gamma alumina framework shifted to higher temperatures in comparison with pure n-OD. In addition, the mass loss of SSCP4 composite was found to be 39.58%, which is coherent with the n-OD content (mass/%) calculated from DSC results. Although char residue (%) of the n-OD at 600 °C was near to zero, SSCP4 indicated higher residual mass due to the presence of nano-gamma alumina framework which was led to decelerate the escape of volatile products during the thermal decomposition step. It could be concluded that obtained higher char residue mass for SSCP4 than this of the n-OD is as a reflection of improvement thermal stability of composite PCMs with thanks to shape-stabilization.

Chemical and morphologic characterization of SSCPs

The chemical characterization of obtained composite SSCP4 besides to n-OD and γ-Al_2O_3 was conducted with FT-IR analysis, and the spectra of samples were given in Fig. 4. As seen from the n-OD spectrum, the absorbance bands at 2953, 2911 and 2847 cm^{-1} could be attributed to the stretching of aliphatic C–H groups. The characteristic peaks for paraffin observed at 1470 cm^{-1}, 1369 cm^{-1} and 716 cm^{-1} are due to C–H bending vibrations, methyl bending vibration and long-chain methyl bending vibration, respectively. As seen in γ-Al_2O_3 spectrum, the peaks at 3412 cm^{-1} and 1635 cm^{-1} were due to stretching and the bending vibrations of OH groups located on the surface of nano-gamma alumina. The bands located at 1378 cm^{-1} and 910 cm^{-1} were due to the stretching and bending vibrations of Al–O. The peak shift observed in the spectrum of SSCP4 between 1200 and 800 cm^{-1} in comparison with spectrum of the γ-Al_2O_3 was due to weak physical interactions between the n-OD and Al–O based on the capillary and surface tension forces. As seen from the Fig. 4, all the characteristic peaks of n-OD and γ-Al_2O_3 were available in SSCP4 spectrum while the any new peak was not observed. This result confirms that n-OD was physically adsorbed into γ-Al_2O_3 scaffold.

Moreover, the impregnation of n-OD into porous γ-Al_2O_3 was investigated by POM analysis. As given in Fig. 5, monitoring of more dark and opaque brownish areas in SSCP4 view in comparison with image of neat transparent γ-Al_2O_3 framework signified well penetration of n-OD into porous supporting material.

Leakage test of SSCPs

Limiting PCM into a framework provides advantages such as reducing exposed to external influences and holding PCM in specific volume. Hereby, testing possible leakage of

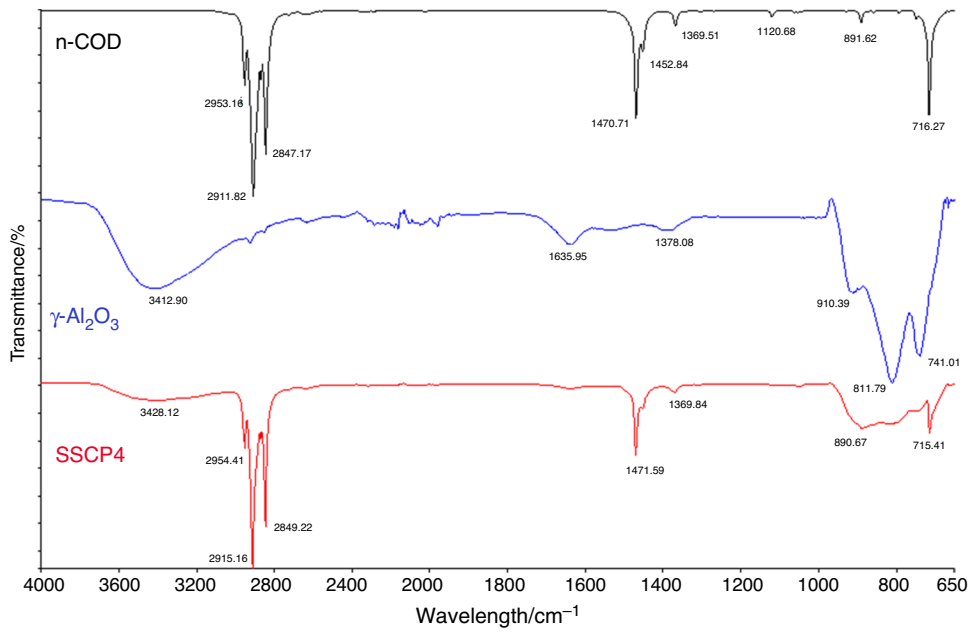

Fig. 4 FT-IR spectra of the n-OD, γ-Al_2O_3 and SSCP4

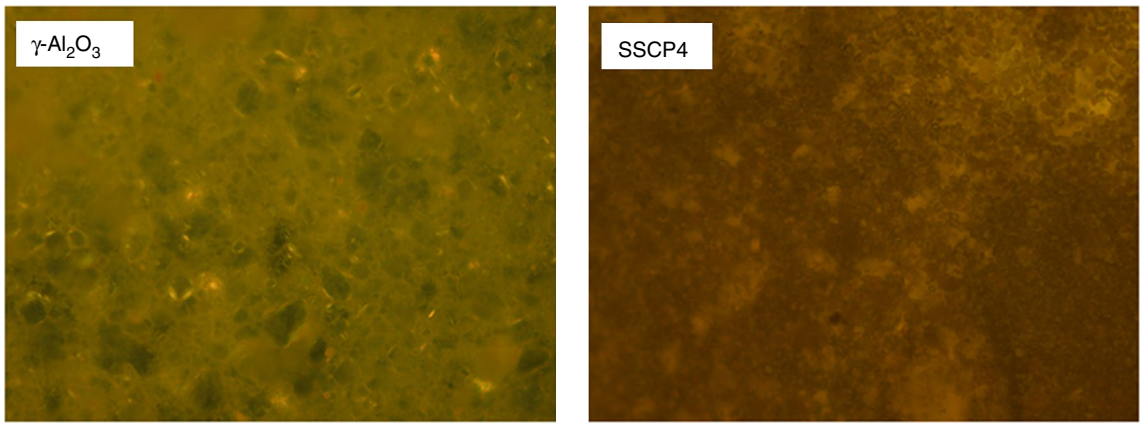

Fig. 5 POM views of nano γ-Al_2O_3 and SSCP4

shape-stabilized PCM is crucial for prevention of problems that will be occurred during the phase transition. SSCPs and n-OD were kept in a vacuum oven tuned at 45 °C ± 5 °C for 2 h, which is higher than melting temperature of n-OD. Then, the test paper placed onto samples and applied pressure in order to check the oily spot formation. As a consequence, all the SSCPs maintained their stability, and there was no leakage of melted n-OD from SSCPs with thanks to the capillary effect and surface tension forces (Fig. 6).

Investigation of thermal behavior of SSCPs

The changes in thermal behavior of SSCP4, n-OD and nano γ-Al_2O_3 framework related with latent heat storage capacity during the cooling process were expressed on Fig. 7. As expected from γ-Al_2O_3 framework, neat porous γ-Al_2O_3 not demonstrated any phase transition due to the absence of PCM in the structure. On the other hand, as noticed from the solidifying curve given in Fig. 7, SSCP4 indicated the phase transition during cooling with thanks to incorporation of n-OD in porous structure of the gamma alumina. However, it could be noticed that SSCP4 started phase transition from liquid to solid state later than pure n-OD. It could be a result of the limitation of n-OD with gamma alumina framework used as a shell material. This result is consistent with DSC results showing that the initial crystallization temperature during cooling of SSCP4 was shifted to lower temperatures compared to pure n-OD.

Thermal reliability of SSCP4 was also tested by exposing to thermal cycle of 100 times with a thermal cycler

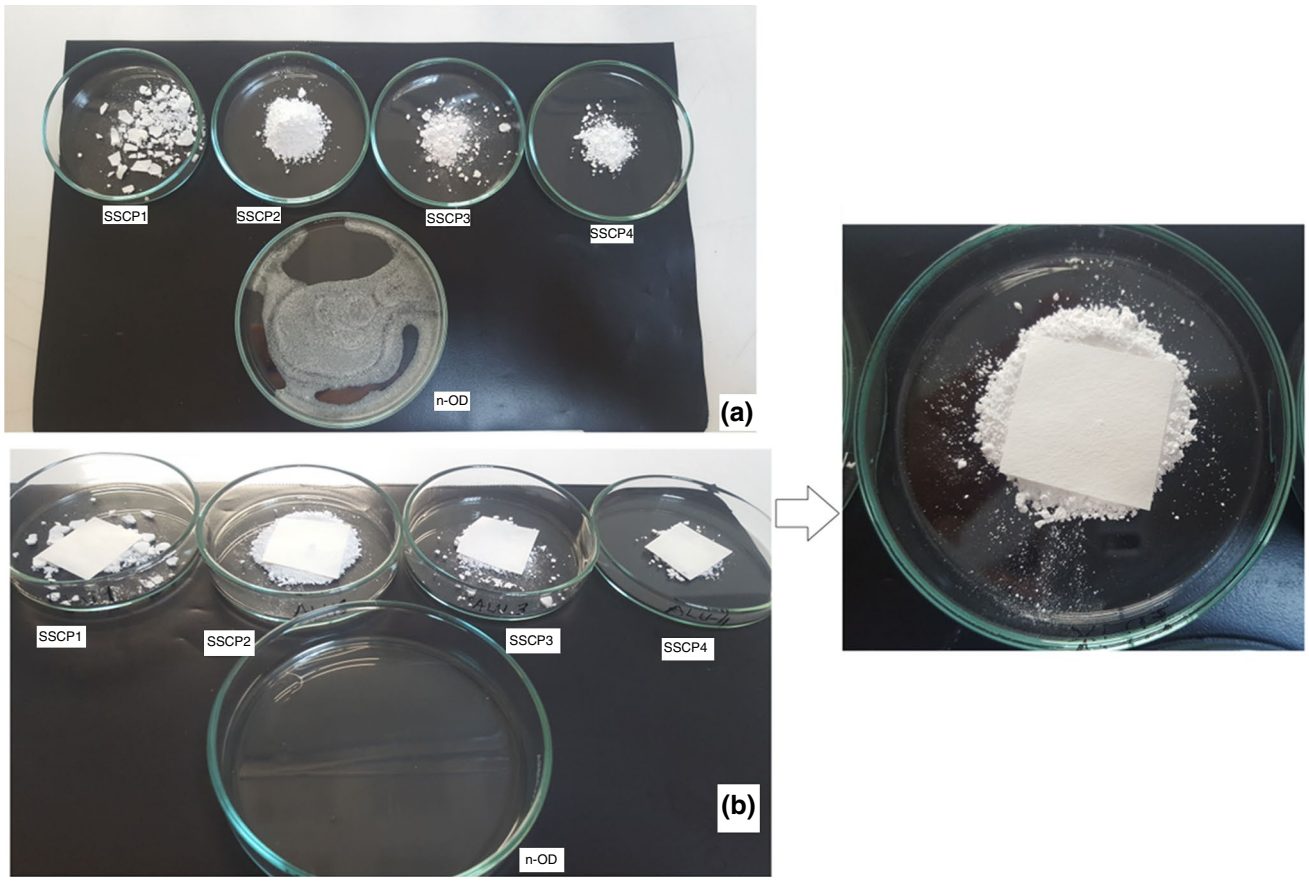

Fig. 6 Leakage test of shape-stabilized composite PCMs (SSCPs): before heating (**a**) and after heating and applying pressure (**b**)

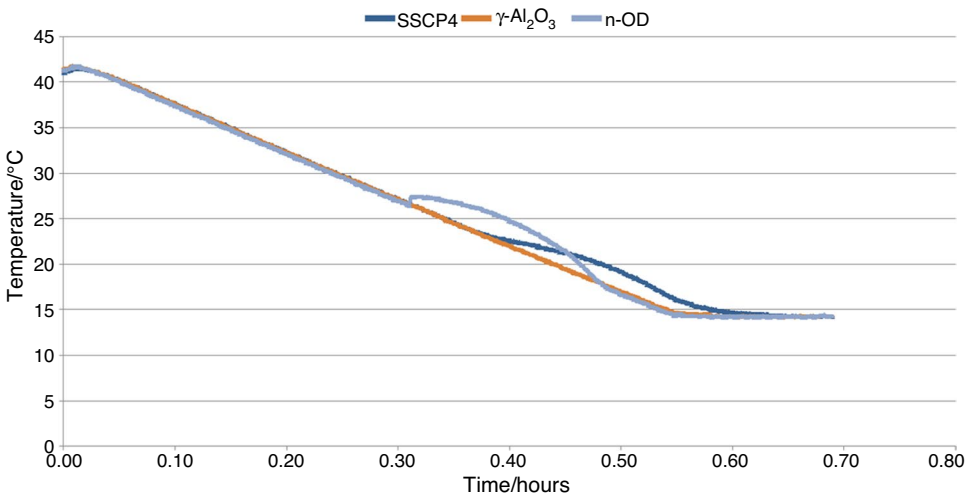

Fig. 7 The heat storage curves of n-OD, γ-Al_2O_3 and SSCP4 during cooling

(BIORAD, T100). DSC curves of SSCP 4 obtained before and after melting–freezing thermal cycling test were given comparatively in Fig. 8, and data were presented in Table 5. As given in Table 5, after thermal cycling test, the temperatures of onset, peak and endset belonging to SSCP4 have changed only 1.34, 0.22 and 0.12 °C, respectively, while the latent heat was found to be 84.45 J g^{-1}. As seen from the Table 5, the decline in magnitude of latent heat is only 1.55 J g^{-1}. This slightly changes within the acceptable range for applications have affirmed the thermal reliability of the composite.

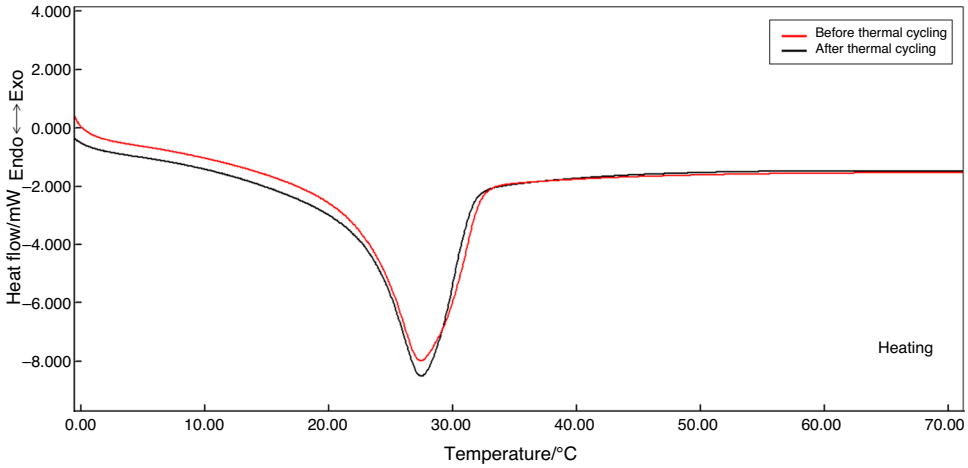

Fig. 8 DSC curves of SSCP4 before and after thermal cycling

Table 5 Phase change properties of SSCP4 before and after thermal cycling

Number of thermal turns	T_{om}/°C	T_{pm}/°C	T_{em}/°C	ΔH_m/J g^{-1d}
0	21.93	27.40	32.34	86.00
100	20.59	27.18	32.22	84.45

Conclusions

A series of shape-stabilized n-OD/nano gamma alumina composite phase change materials were successfully prepared by one step impregnation method and characterized. n-OD was used as PCM while the nano-sized gamma alumina employed as framework. Based on the DSC results that SSCP4 was found to be the composite which has the highest latent heat storage capacity (86.00 J g^{-1}) as a consequence of having the highest n-OD content (39.09 mass/%). Moreover, the melting and crystallization peak temperatures of SSCP4 were found to be 27.40 and 18.95 °C, respectively. Additionally, based on the TGA result thermal stability of SSCP4 was not only improved but also form stability was performed, which was checked out with leakage test on account of the providing of shape-stabilization with alumina template. It could be concluded that the composite of SSCP4 is a good candidate for low temperature thermal storage applications such as the maintaining thermal comfort in buildings or solar thermal energy storage systems.

References

1. Mert HH. PolyHIPE composite based form stable phase change material for thermal energy storage. Int J Energy Res. 2020;44:6583–94. https://doi.org/10.1002/er.5390.
2. Kheradmand M, Abdollahzadeh M, Abdollahzadeh M, Azenha M, De Aguiar, JLB. Phase change materials as smart nanomaterials for thermal energy storage in buildings. In: Tiwari A, Mishra YK, Kobayashi H, Turner APF, editors. Intelligent Nanomaterials; 2016. p. 249–93. doi: https://doi.org/10.1002/9781119242628.ch9
3. Chao W, Yang H, Cao G, Sun X, Wang X, Wang C. Carbonized wood flour matrix with functional phase change material composite for magnetocaloric-assisted photothermal conversion and storage. Energy. 2020;202:117636. https://doi.org/10.1016/j.energy.2020.117636.
4. Ren M, Liu Y, Gao X. Incorporation of phase change material and carbon nanofibers into lightweight aggregate concrete for thermal energy regulation in buildings. Energy. 2020;197:117262. https://doi.org/10.1016/j.energy.2020.117262.
5. Ren W, Cao L, Zhang D. Composite phase change material based on reduced graphene oxide/expanded graphite aerogel with improved thermal properties and shape-stability. Int J Energy Res. 2020;44:242–56. https://doi.org/10.1002/er.4900.
6. Umair MM, Zhang Y, Iqbal K, Zhang S, Tang B. Novel strategies and supporting materials applied to shape-stabilize organic phase change materials for thermal energy storage – a review. Appl Energy. 2019;235:846–73. https://doi.org/10.1016/j.apenergy.2018.11.017.
7. Sarı A, Hekimoglu H, Tyagi VV, Sharma RK. Evaluation of pumice for development of low-cost and energy-efficient composite phase change materials and lab-scale thermoregulation performances of its cementitious plasters. Energy. 2020;207:118242. https://doi.org/10.1016/j.energy.2020.118242.
8. Zhang P, Meng ZN, Zhu H, Wang YL, Peng SP. Melting heat transfer characteristics of a composite phase change material fabricated by paraffin and metal foam. Appl Energy. 2017;185:1971–83. https://doi.org/10.1016/j.apenergy.2015.10.075.
9. Xiao X, Zhang P, Li M. Preparation and thermal characterization of paraffin/metal foam composite phase change material. Appl Energy. 2013;112:1357–66. https://doi.org/10.1016/j.apenergy.2013.04.050.
10. Fleming E, Wen S, Shi L, Silva AK. Experimental and theoretical analysis of an aluminum foam enhanced phase change thermal storage unit. Int J Heat Mass Transf. 2015;82:273–81. https://doi.org/10.1016/j.ijheatmasstransfer.2014.11.022.
11. Mert MS, Mert HH, Sert M. Microencapsulated oleic–capric acid/hexadecane mixture as phase change material for thermal energy storage. J Therm Anal Calorim. 2019;136:1551–61. https://doi.org/10.1007/s10973-018-7815-5.
12. Mert MS, Mert HH, Sert M. Investigation of thermal energy storage properties of a microencapsulated phase change material

using response surface experimental design methodology. Appl Therm Eng. 2019;149:401–13. https://doi.org/10.1016/j.applthermaleng.2018.12.064.
13. Su W, Darkwa J, Kokogiannakis G. Review of solid–liquid phase change materials and their encapsulation technologies. Renew Sust Energy Rev. 2015;48:373–91. https://doi.org/10.1016/j.rser.2015.04.044.
14. Karthikeyan M, Ramachandran T. Review of thermal energy storage of micro- and nanoencapsulated phase change materials. Mater Res Innov. 2014;18(7):541–54. https://doi.org/10.1179/1433075X13Y.0000000143.
15. Jebasingh BE, Arasu AV. A comprehensive review on latent heat and thermal conductivity of nanoparticle dispersed phase change material for low-temperature applications. Energy Storage Mater. 2020;24:52–74. https://doi.org/10.1016/j.ensm.2019.07.031.
16. Ho CJ, Gao JY. Preparation and thermophysical properties of nanoparticle-in-paraffin emulsion as phase change material. Int Commun Heat Mass Transf. 2009;36:467–70. https://doi.org/10.1016/j.icheatmasstransfer.2009.01.015.
17. Fang G, Li H, Cao L, Shan F. Preparation and thermal properties of form-stable palmitic acid/active aluminum oxide composites as phase change materials for latent heat storage. Mater Chem Phys. 2012;137:558–64. https://doi.org/10.1016/j.matchemphys.2012.09.058.
18. Wei H, Li X. Preparation and characterization of a lauric-myristic-stearic acid/Al2O3-loaded expanded vermiculite composite phase change material with enhanced thermal conductivity. Sol Energy Mater Sol Cells. 2017;166:1–8. https://doi.org/10.1016/j.solmat.2017.03.003.
19. Zhao L, Wang H, Luo J, Liu Y, Song G, Tang G. Fabrication and properties of microencapsulated n-octadecane with TiO_2 shell as thermal energy storage materials. Sol Energy. 2016;127:28–35. https://doi.org/10.1016/j.solener.2016.01.018.
20. Mert MS, Mert HH, Yılmaz C. Preparation and characterization of paraffin microcapsules for energy saving applications. J Appl Polym Sci. 2019;136:47874. https://doi.org/10.1002/app.47874.
21. Mert HH, Mert MS. Preparation and characterization of encapsulated phase change materials in presence of gamma alumina for thermal energy storage applications. Thermochim Acta. 2019;681:178382. https://doi.org/10.1016/j.tca.2019.178382.
22. Ambroz F, Macdonald TJ, Martis V, Parkin IP. Evaluation of the BET theory for the characterization of meso and microporous MOFs. Small Methods. 2018;2:1800173. https://doi.org/10.1002/smtd.201800173.
23. Gao J, Tao W, Chen D, Guo X, Chen Y, Jiang Y. High performance shape-stabilized phase change material with nanoflower-likewrinkled mesoporous silica encapsulating polyethylene glycol: preparation and thermal properties. Nanomaterials. 2018;8:385. https://doi.org/10.3390/nano8060385.
24. Han J, Liu S. Myristic acid-hybridized diatomite composite as a shape-stabilized phase change material for thermal energy storage. RSC Adv. 2017;7:22170. https://doi.org/10.1039/C7RA02385E.
25. Feng L, Zheng J, Yang H, Guo Y, Li W, Li X. Preparation and characterization of polyethylene glycol/active carbon composites as shape-stabilized phase change materials. Sol Energy Mater Sol Cells. 2011;95(2):644–50. https://doi.org/10.1016/j.solmat.2010.09.033.
26. Khadiran T, Hussein MZ, Zainal Z, Rusli R. Shape-stabilised n-octadecane/activated carbon nanocomposite phase change material for thermal energy storage. J Taiwan Inst Chem Eng. 2015;55:189–97. https://doi.org/10.1016/j.jtice.2015.03.028.
27. Fang X, Zhang Z, Chen Z. Study on preparation of montmorillonite-based composite phase change materials and their applications in thermal storage building materials. Energy Convers Manag. 2008;49(4):718–23. https://doi.org/10.1016/j.enconman.2007.07.031.
28. Li C, Xie B, Chen J. Graphene-decorated silica stabilized stearic acid as a thermal energy storage material. RSC Adv. 2017;7:30142–51. https://doi.org/10.1039/C7RA05204A.
29. Ramakrishnan S, Sanjayan J, Wang X, Alam M, Wilson J. A novel paraffin/expanded perlite composite phase change material for prevention of PCM leakage in cementitious composites. Appl Energy. 2015;157:85–94. https://doi.org/10.1016/j.apenergy.2015.08.019.
30. Li M, Wu Z, Kao H, Tan J. Experimental investigation of preparation and thermal performances of paraffin/bentonite composite phase change material. Energy Convers Manag. 2011;52(11):3275–328. https://doi.org/10.1016/j.enconman.2011.05.015.
31. Karaipekli A, Sarı A. Capric–myristic acid/vermiculite composite as form-stable phase change material for thermal energy storage. Sol Energy. 2009;83(3):323–32. https://doi.org/10.1016/j.solener.2008.08.012.
32. Li C, Yu H, Song Y, Wang M, Liu Z. A n-octadecane/hierarchically porous TiO2 form-stable PCM for thermal energy storage. Renew Energy. 2020;145:1465–73. https://doi.org/10.1016/j.renene.2019.06.070.
33. Liu Y, Xia Y, An K, Huang C, Cui W, Wei S, Ji R, Xu F, Zhang H, Sun L. Fabrication and characterization of novel meso-porous carbon/n-octadecane as form-stable phase change materials for enhancement of phase-change behaviour. J Mater Sci Technol. 2019;35(5):939–45. https://doi.org/10.1016/j.jmst.2018.11.001.
34. Atinafu DG, Yun BY, Wi S, Kang Y, Kim S. A comparative analysis of biochar, activated carbon, expanded graphite, and multi-walled carbon nanotubes with respect to PCM loading and energy-storage capacities. Environ Res. 2021;195:110853. https://doi.org/10.1016/j.envres.2021.110853.
35. Hekimoğlu G, Nas M, Ouikhalfan M, Sarı A, Tyagi VV, Sharma RK, Kurbetci S, Saleh TA. Silica fume/capric acid-stearic acid PCM included-cementitious composite for thermal controlling of buildings: Thermal energy storage and mechanical properties. Energy. 2021;219:119588. https://doi.org/10.1016/j.energy.2020.119588.